INTERNATIONAL JOURNAL OF CLIMATOLOGY
Int. J. Climatol. (2014)
Published online in Wiley Online Library
(wileyonlinelibrary.com) DOI: 10.1002/joc.4230

RMetS
Royal Meteorological Society

Short Communication

Tree-ring reconstructed temperature index for coastal northern Japan: implications for western North Pacific variability

Rosanne D'Arrigo,[a]* Rob Wilson,[a,b] Greg Wiles,[a,c] Kevin Anchukaitis,[a,d] Olga Solomina,[a,e] Nicole Davi,[a,f] Clara Deser[g] and Ekaterina Dolgova[e]

[a] *Tree-Ring Laboratory, Lamont-Doherty Earth Observatory, Palisades, NY, USA*
[b] *Department of Geography and Geosciences, University of Saint Andrews, UK*
[c] *Department of Geology, The College of Wooster, OH, USA*
[d] *Department of Geology and Geophysics, Woods Hole Oceanographic Institute, MA, USA*
[e] *Institute of Geography, Russian Academy of Sciences, Moscow, Russia*
[f] *Department of Environmental Science, William Patterson University, NJ, USA*
[g] *Climate and Global Dynamics, NCAR, Boulder, CO, USA*

ABSTRACT: While paleoclimatic studies have extended our understanding of North Pacific climate variability, these have been almost exclusively based on proxies from western North America. We present a tree-ring reconstruction of June to September coastal air temperatures for Nemuro, northeastern Japan for the past four centuries. It explains 36% of the variance in instrumental temperatures and correlates significantly with indices of the atmosphere–ocean circulation. Spectral analyses reveal robust bidecadal peaks that appear associated with regional modes of western North Pacific variability. At decadal time scales, Nemuro temperatures appear to be influenced by the confluence of the Kuroshio and Oyashio currents, a primary centre of action driving Pacific Decadal Variability. Regime shifts (e.g. 1976) are weakly expressed relative to western North America. These aspects of western North Pacific climate are regionally distinct relative to those elsewhere in the basin, with greater complexity than can be attributed to the Pacific Decadal Oscillation (PDO) alone.

KEY WORDS western North Pacific; dendrochronology; Japan; tree rings; temperature reconstruction

Received 8 August 2014; Revised 3 November 2014; Accepted 6 November 2014

1. Introduction

North Pacific climate variability influences marine and terrestrial ecosystems and human populations around the North Pacific rim (Mantua *et al.*, 1997). Atmosphere–ocean phenomena linked to the Pacific Decadal Oscillation (PDO), the dominant mode of sea surface temperature (SST) variability in the North Pacific Ocean, have been shown to be a strong control on temperature and precipitation over adjacent land areas (Mantua *et al.*, 1997). However, there is much greater complexity inherent in North Pacific climate variability on interannual to decadal and longer time scales than only the PDO (Deser *et al.*, 2004; Schneider and Cornuelle, 2005). We use annual tree-ring records to reconstruct temperatures for northeastern Japan, a region highly sensitive to western North Pacific climate variability. In so doing, we show that long-term North Pacific climate patterns and variability are substantially more complex than can be gleaned from any single indicator such as the PDO, particularly with respect to the western side of the basin (Bond *et al.*, 2003).

Fluctuations in North Pacific climate have been observed in the instrumental record on interannual to multidecadal time scales. A key example is the Pacific regime shift in 1976, which was associated with an abrupt transition from a negative to positive PDO phase, with related impacts on marine and land ecosystems (Mantua *et al.*, 1997). This shift was linked to widespread warming along the coast of western North America, with a deepened and eastward-shifted Aleutian Low. To a lesser extent, it was associated with cooling in the western North Pacific. Earlier shifts occurred in ∼1924 (from negative to positive phase), and ∼1946 (from positive to negative) (Mantua *et al.*, 1997; D'Arrigo *et al.*, 2005). The latter event was linked to SST and surface air warming centred strongly over Japan during the colder months (Minobe, 1997, 1999; Deser *et al.* 2004). Other regime shifts have been proposed for 1988/1989 and the late 1990s (Bond *et al.* 2003). Such Pacific multidecadal mechanisms, their origins and their potential causes (e.g. tropical forcing – Deser *et al.*, 2004;

* Correspondence to: R. D'Arrigo, Tree-Ring Laboratory, Lamont-Doherty Earth Observatory, Palisades 10964, New York, USA.
E-mail: rdd@ldeo.columbia.edu

D'Arrigo *et al.*, 2005; Wang *et al.*, 2012a) are not well understood due to the limited length of instrumental data. Minobe (1999) theorized that these shifts result from interaction between bidecadal and pentadecadal modes of circulation, but this theory appears to break down when tested over the last millennium (Wilson *et al.*, 2007). It is perhaps more likely that the apparent regime shifts are due to the random superposition of multiple independent processes and may thus not represent a single physical phenomenon (Newman, 2007; Wang *et al.*, 2012b).

In contrast to western North America, relatively few studies have investigated the climate of the western North Pacific sector and its distinct regional characteristics. The Subarctic Front, Okhotsk High, Kuroshio–Oyashio Extension (KOE) and East Asian monsoon are distinct physical features of this region's circulation, climate and geography. The Subarctic Front east of Japan (defined as SST averaged over 34°–48°N, 150°–180°E) features the most intense temperature gradient in the Pacific basin, extending zonally to 42°N, where cool water from the Oyashio current (OC) joins warm water in the Kuroshio Extension (Nakamura *et al.*, 1997). An above-average Okhotsk High [sea level pressure (SLP), averaged over 50°–60°N, 140°–160°W] is linked with cool summers in northern Japan and vicinity (Ogi *et al.*, 2004). There is also increasing evidence that Eurasian climate plays a critical role in such variability (Frauenfeld and Davis, 2002; Nakamura *et al.*, 2002), including the effects of the Siberian High (SH) pressure cell. These observations illustrate some of the unique and complex features of the climate of the western North Pacific sector.

Longer time series, gleaned from precisely dated paleoclimatic records, can aid considerably in understanding the basic mechanisms that drive climate variability across the North Pacific, particularly on time scales beyond those resolvable in the instrumental record. For western North America, tree rings from the mountain ranges along the Gulf of Alaska (GOA) and other locations were used to generate reconstructions of North Pacific climate linked to the PDO (e.g. D'Arrigo *et al.*, 2001, 2005; Gedalof and Smith, 2001; Wiles *et al.*, 2014a). Building on these and other prior studies, Wilson *et al.* (2007) described a 1300-year tree-ring reconstruction of GOA January to September coastal air temperatures, identifying statistically significant spectral peaks in North Pacific climate, and outlining evidence for multiple regime shifts over time.

On the western side of the North Pacific basin, however, tree-ring research has been much more limited, but this situation has recently improved. This work includes individual-site tree-ring investigations in northern coastal Japan [Hokkaido (D'Arrigo *et al.*, 1997; Davi *et al.*, 2001)], the Russian Far East [Kurile Islands (Jacoby *et al.*, 2004), Kamchatka (Solomina *et al.*, 2007; Sano *et al.*, 2010) and Sakhalin (Wiles *et al.*, 2014b)], Japan and Korea (Ohyama *et al.*, 2013). Cook *et al.* (2012) reconstructed temperatures for temperate East Asia, focusing mainly on continental climate. D'Arrigo and Wilson (2006) reconstructed the Asian expression of the spring PDO, which identified significant regime shifts similar to those in the instrumental period, although distinct features reflecting local and regional response to volcanic events and the El Niño-Southern Oscillation (ENSO) were noted. Other reconstructions of the PDO have been developed from Asia based on historical rainfall records (Shen *et al.*, 2006), and corals from the South China Sea (Deng *et al.*, 2013).

2. Data and methods

We use a network of tree-ring chronologies (Table 1, Figure 1) from the Russian Far East and Japan to reconstruct northern Japanese coastal air temperatures over the past four centuries. We target this region because it is particularly sensitive to northwestern Pacific maritime climate, and is potentially impacted by the Subarctic Front, KOE and other aspects of northwestern Pacific circulation with features distinct from those observed in either the eastern northern Pacific or interior Asia.

Our tree-ring reconstruction of coastal summer surface air temperatures is based on the meteorological station record at Nemuro, northeastern Japan [Figure 1, 43.33°N, 145.58°E, elevation 39 m, Global Historical Climate Network (GHCN); Peterson and Vose, 1997]. This station is situated on a narrow peninsula that extends eastward into the North Pacific Ocean from the island of Hokkaido. We selected this station for analysis because it is considerably longer than any other records in the region (beginning in 1880), allowing for longer intervals for model calibration and verification (Cook and Kairiukstis, 1990). Importantly, it is located at the northwestern edge of the region of peak correlation of land-based summer surface air temperatures and SSTs with the PDO and related indices, thus providing important information on western North Pacific climate and atmosphere–ocean circulation (Figures 1 and 2). It is in this region that the OC to the north meets the Kuroshio current (KC) from the south, representing the KOE and Arctic Front (Nakamura *et al.*, 1997).

Nemuro is also in close proximity to several of our individual tree-ring sites developed over the past few decades, and these records respond positively to summer temperatures during the growing season (Figure 1, Table 1). Figure 2(a) shows the spatial correlation pattern of Nemuro with summer land/sea temperatures for the region. All tree-ring sites used in our reconstruction are situated within the region of positive correlation. Likewise, they all sit within an area of broad, negative correlation between the PDO and summer temperature over northern Japan (including Nemuro) and the southern Russian Far East (Figure 2(b)). This association is weaker over Japan during the winter to spring seasons (February to May), when the area of strongest correlation appears to shift eastward (Figure 2(c)), and when the positive PDO/temperature relationship is much stronger over western America.

A network of six tree-ring chronologies was used as a set of candidate predictors in principal components regression (PCR) modelling (Cook and Kairiukstis, 1990)

Table 1. Site information for six tree-ring chronologies used to reconstruct Nemuro, Japan June to September temperatures. Also shown are their correlations (all significant at or above the 0.05 level) with Nemuro instrumental temperatures based on the 1900–1993 calibration period, and beta coefficients. All are ring-width records except for Asahikawa, which is maximum latewood density (MXD).

Site location	Country	Length	Latitude	Longitude	Correlation	Beta coefficient	Tree species
Chamga, Sakhalin	Russia	1620–2004	51°01′48″N	143°35′24″E	0.37	0.27	*Larix* spp.
Kunashir, Kuriles	Russia	1610–2000	43°52′47″N	145°36′24″E	0.49	0.15	*Quercus crispula*
Asahikawa, Hokkaido (MXD)	Japan	1640–1997	43°46′12″N	142°33′E	0.23	0.05	*Picea glehnii*
Saroma, Hokkaido	Japan	1700–1993	43°48′N	142°20′E	0.23	0.09	*Quercus dentata*
Tokachi, Hokkaido	Japan	1520–1997	43°30′N	143°12′E	0.22	0.19	*Picea* spp.
Omebetsu, Hokkaido	Japan	1580–1998	43°13′N	145°28′E	0.49	0.21	*Picea* spp.

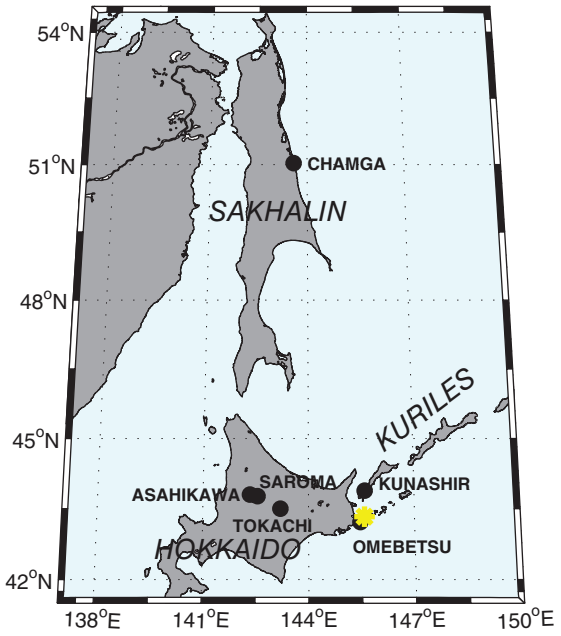

Figure 1. Map showing locations of the tree-ring sites used in this reconstruction and the Nemuro (*) meteorological station. The islands of Hokkaido, Sakhalin and the Kuriles are also labelled.

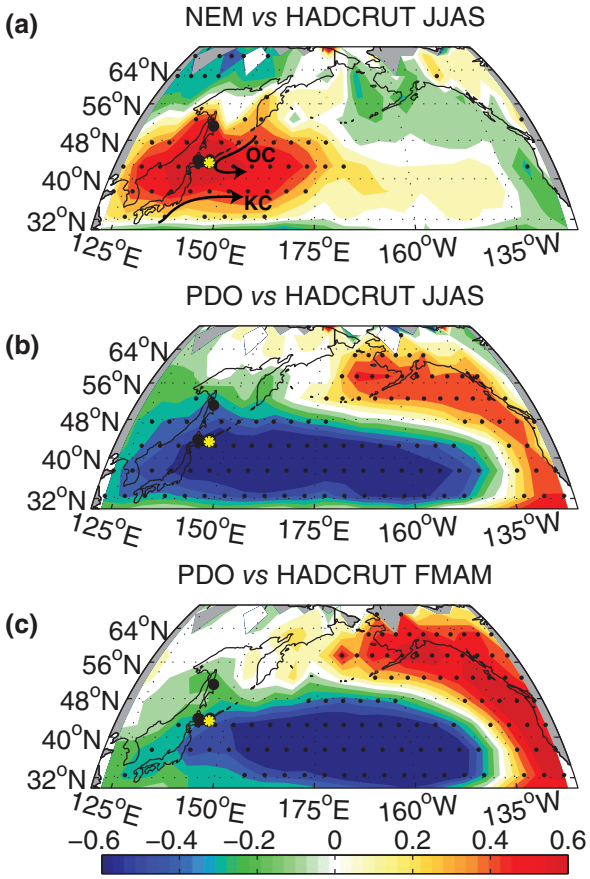

Figure 2. (a) Spatial correlation maps for 1900–1993 comparing the Nemuro, Japan meteorological station temperature data (*) and gridded HADCRUT land/sea temperatures (Morice *et al.*, 2012) for the June to September season. Large black dots denote the six tree-ring sites (see Table 1, Figure 1) used in the reconstruction. (b) As in (a), but between the PDO index (1900–2012) and the HADCRUT data for the June to September season. (c) As in (b), but for the February to May season. Kuroshio–Oyashio Currents/Extension also shown by arrows. Nemuro is near the confluence of these currents.

to reconstruct northern Japanese temperatures over the past several centuries. These chronologies are based on wood collections from living trees that mainly show sensitivity to temperature. The sites are from coastal and near coastal regions impacted significantly by North Pacific climate. These data include chronologies developed by the Tree-Ring Laboratory-Lamont-Doherty Earth Observatory (TRL-LDEO) and collaborators, and several donated by contributors to the NOAA Paleoclimatology International Tree-Ring Data Bank (ITRDB) and other sources. We include only those records that expressed significant agreement with the Nemuro record and which were situated within the 'zone of coherence' identified between the PDO and HADCRU data shown in Figure 2(b). The records used herein were mainly from maritime sites situated closest to the Nemuro station (Table 1, Figure 1). Five series are based on ring width; one, for Hokkaido, is maximum latewood density or MXD (Davi *et al.*, 2001). Four are of coniferous species of spruce and larch, and two of oak (Table 1). Several were utilized in prior local to regional studies (e.g. D'Arrigo *et al.*, 1997, 2005; Davi *et al.*, 2001; Jacoby *et al.*, 2004; D'Arrigo and Wilson, 2006; Cook *et al.*, 2012; Wiles *et al.*, 2014b), whereas others have not been previously published. Data were detrended using standard methods (e.g. negative exponential or straight line/regression functions, to remove non-climatic biological age-related trends), with the

Table 2. Correlations between Nemuro, Japan instrumental and reconstructed June to September temperatures and indices of the PDO, West Pacific pattern (http://www.cpc.ncep.noaa.gov/data/teledoc/wp.shtml), Arctic Front, Okhotsk High, KOE and Enoshima, Japan SST. First difference comparisons in parentheses. The first difference in this context refers to the value of a time series at time *t* minus the series at time *t*-1 (Cook and Kairiukstis, 1990). Arctic Front: SST averaged over 34°–48°N, 150°–180°E; Okhotsk High Index averaged over 50°–60°N, 140°–160°E; KOE Index of SST averaged over 35°–45°N, 140°–180°E, Enoshima, Japan SST averaged over 38°–39°N, 141°–142°E. Although the JJAS season was used for all of these comparisons, correlations can be higher for individual months and datasets. For the Okhotsk High, for example, values are much higher for June alone: −0.44 for the reconstruction.

Nemuro data	Indices					
	PDO	W. Pacific Index	Arctic Front Index	Okhotsk High Index	Kuroshio Extension Index	Enoshima Index
Tree-ring reconstruction	−0.40 (−0.49)	0.59 (0.54)	0.33 (0.40)	−0.26 (−0.36)	0.49 (0.57)	0.16 (0.23)
	0.0001 (0.0000)	0.000 (0.0002)	0.0002 (0.0000)	0.0018 (0.0000)	0.0000 (0.0000)	0.0813 (0.0091)
	n 94 (93)	n 44 (43)	n 124 (123)	n 144 (143)	n 104 (100)	n 124 (123)
Instrumental temperatures	−0.52 (−0.63)	0.37 (0.52)	0.55 (0.57)	−0.27 (−0.42)	0.67 (0.71)	0.47 (0.48),
	0.000, (0.0000)	0.0000 (0.0000)	0.0000 (0.0000)	0.0017 (0.0000)	0.0000 (0.0000)	0.0000 (0.0000)
	n 114 (113)	n 64 (63)	n 134 (133)	n 134 (133)	n 123 (119)	n 134 (133)

caveat that a certain amount of secular variability will be removed related to mean sample length (Cook and Kairiukstis, 1990). We therefore focus herein on the annual to multidecadal variability in Pacific climate gleaned from these tree-ring records.

Climate analyses were performed using the HADISST (Rayner *et al.*, 2003), HADCRUT land/sea temperatures (Morice *et al.*, 2012), HADSST3 (Kennedy *et al.*, 2011) and HADISLP (Allan and Ansell, 2006) data sets. The strongest overall correlations were found for the June to September (JJAS) summer season based on iterative PCR model trials. This result differs from that of D'Arrigo and Wilson (2006), who reconstructed the PDO based on a much larger data set (including not only some of the chronologies used herein, but also tree-ring data from mainland north Asia), with March–April–May as their optimal target season. Correlations with Nemuro summer temperatures were positive in sign for all six chronologies. Correlations were strongest for the Kunashir and Omebetsu, Japan chronologies, which are situated closest to Nemuro, within a region where temperatures are well correlated with the PDO and related indices (Tables 1 and 2, Figures 1 and 2, Jacoby *et al.*, 2004). The significance of interannual correlations was evaluated using the method described by Dawdy and Matalas (1964) to account for temporal autocorrelation. For correlation between smoothed series, we used the simulation method described by Ebisuzaki (1997) to estimate significance.

A nested procedure (Cook *et al.* 2002), in which the number of chronologies declines back in time, was used to optimize the length of the reconstruction. Iterative nests begin in 1560, 1590, 1640, 1650, 1700 and 1710. The final reconstruction was developed by splicing these nested series together after their variance and mean had been adjusted to that of the best-replicated 1710–1993 nest. This was done in order to avoid any changes in variance in the overall reconstruction due to weakening of the modelled signal back/forward in time. For each model nest, we used 1900–1993 as the calibration period and 1880–1899 as the period of independent verification.

Figure 3(a) shows the observed and estimated June to September Nemuro temperatures for the 1900–1993 calibration period for the best replicated recent period or nest, based on all six chronologies. The level of temperature variance (adjusted r^2) explained by the regression model over the common 1900–1993 calibration period for the most replicated nest is 36%. The calibration period root mean square error (RMSE, Cook and Kairiukstis, 1990) was utilized to derive error estimates for the reconstruction back through time. The full temperature reconstruction based on spliced model nests spans from 1640 to 1993 (Figure 3(b)). The strength of the models declines back in time as chronologies leave the data matrix (Figure 3(c)), with the ar^2 values ranging as low as 14% for the early 1640 model nest (note that earlier nests were truncated although they retained some model skill), based on only three chronologies, indicating that additional long tree-ring records are needed to improve model reliability prior to this time. The nested regression models all passed the rigorous coefficient of efficiency (CE) test (Figure 3(d), indicating predictive skill – Cook and Kairiukstis, 1990), and model residuals show no significant autocorrelation (Figure 3(c)).

3. Results and discussion

The Nemuro temperature reconstruction reveals annual to multidecadal variability in western North Pacific climate over the past four centuries (Figure 3). Unlike other reconstructions for western North America, where the PDO signal is typically much stronger (Wilson *et al.*, 2007; Figure 3), the Nemuro reconstruction does not show clear evidence for the three 20th century major regime shifts identified in the cold season and annual PDO (Mantua *et al.*, 1997; Sano *et al.*, 2010). This is particularly true for the two most recent transitions (1946 and 1976), and the

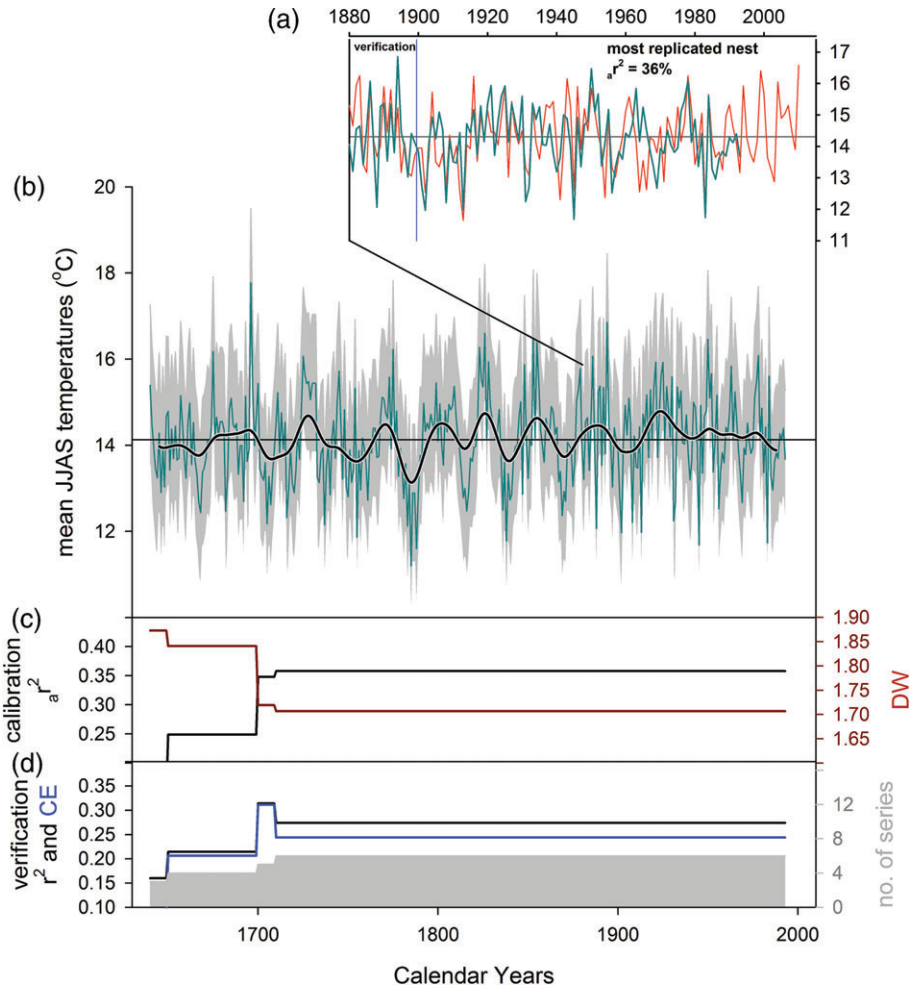

Figure 3. (a) Nemuro, Japan observed (red in online) and reconstructed (green in online) JJAS temperatures based on western North Pacific tree rings for most replicated nest and full calibration period from 1900–1993. (b) full Nemuro temperature reconstruction over 1640–1993 with 2-sigma error bars. Smoothed line is a 28-year spline function; (c) Calibration ar^2 and Durbin-Watson (DW) statistic results for the 1900–1993 period for each nest; (d) Verification (1880–1899) r^2 and CE values for each nest. Calibration and verification r^2 values refer to the levels of variance explained by the tree-ring data in regression analysis (Cook and Kairiukstis, 1990).

summer instrumental data from Nemuro likewise fails to indicate abrupt transitions at these times. These observations are largely explained by the fact that the trees respond primarily to summer conditions, whereas the PDO is most strongly expressed in the colder months, and in the eastern North Pacific sector. This point is illustrated in Figure 4, which shows spatial anomaly maps comparing the difference in temperature for the 10 years before and after 1976. The 'classic' PDO spatial pattern is clear, particularly for the FMAM season, but it is only weakly expressed for the Nemuro region by summer. An intervention analysis (not shown) identifies a significant shift in the Nemuro FMAM time-series at 1988, although not in 1976. This shift may be related to the Arctic Oscillation, which underwent a substantial change in 1988/1989 coinciding with strong warming over northern Japan (Thompson and Wallace, 1998). There is no evidence of a significant change in temperature for the Nemuro region for the reconstructed JJAS season in 1988, nor for the mid-1940s shift, believed to be the strongest in the instrumental record over Japan (Nakamura *et al.*, 1997), at least in the colder months.

To further investigate the large-scale climatic signal in the Nemuro data, we compare the Nemuro data to six indices of North Pacific atmosphere–ocean circulation (Table 2): (1) the PDO index (Mantua *et al.*, 1997), (2) the West Pacific index (indicator of intensity of the East Asian jet stream – Barnston and Livezey, 1987), (3) the North Pacific Subarctic Frontal Zone index (a region of sharp gradients in SST near the Oyashio–Kuroshio boundary, 34°–48°N, 150°–180°E), (4) the Okhotsk High index (a semi-permanent SLP system over the Okhotsk Sea in warmer months; 50°–60°N, 140°–160°E), (5) the Kuroshio Extension SST index (35°–45°N, 140-180°E) and (6) the Enoshima index of SST, considered a proxy of Oyashio southward penetration along the Japanese coast (Minobe, 1997). Nemuro temperatures are most significantly correlated with these indices during the warm season months, when they are linked to conditions over northern Japan.

The Nemuro reconstruction provides an opportunity to analyse long-term variability, including spectral properties, in western North Pacific climate. Multi-taper method

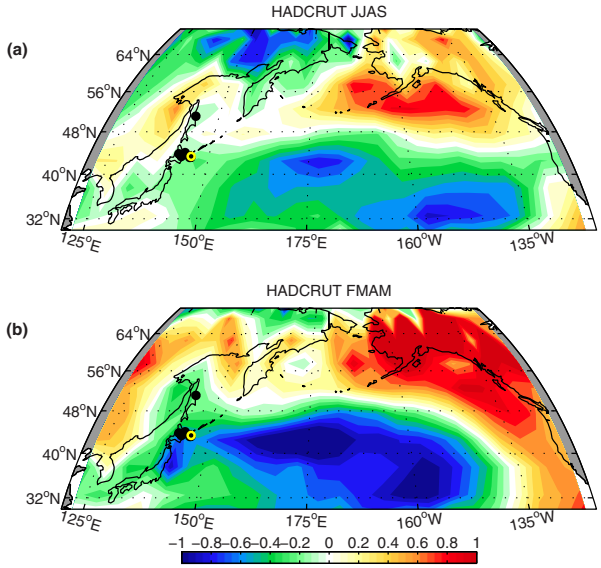

Figure 4. Spatial difference plot (°C) for the 10 years on either side of 1976 (1966 to 1975 *vs* 1977 to 1986) using the HADCRUT temperature data set for the JJAS and FMAM seasons.

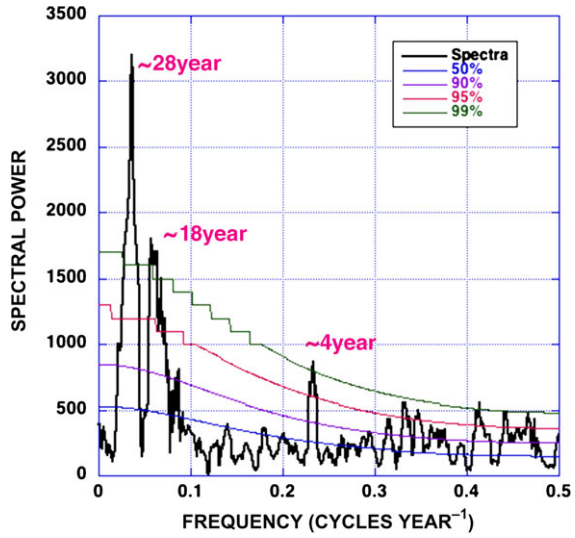

Figure 5. MTM spectral analysis results for Nemuro temperature reconstruction over its length from 1640–1993, showing robust (99% level) peaks centered at ~28 years, 18 and 4 years. Levels of significance shown (null, 90, 95 and 99%).

(MTM) spectral analysis (Thomson, 1982; Mann and Lees, 1996) performed on the reconstruction over 1640–1997 (Figure 5) reveals a robust (above 99% level) peak centred at ~28 years, with another peak, also significant above the 99% level, at ~18 years. There is a ~4-year peak that is within the ENSO bandwidth. While the causes of these modes are not well known, winter SST anomalies for the KOE do show a spectral power at 20–30 years (Pierce *et al.*, 2001). Dominant peaks in the Community Climate System Model (CCSM) KOE SST index have also been described at 15–20 years (Kwon and Deser, 2007). KOE SST anomalies were shown to occur within a period of 18.6 years, with warmer SSTs linked to strong tidal mixing induced by anomalous circulation around the Kurile Straits, with resulting SST and SLP patterns similar to the PDO that can significantly impact Pacific climate (Osafune and Yasuda, 2006; Yasuda *et al.*, 2006; Hasumi *et al.*, 2008; Tanaka *et al.*, 2012). KOE variability impacts extratropical storm tracks and the surface wind stress curl across the North Pacific basin with clearly defined decadal modulations, exerting major influences on western North Pacific climate and ecosystems (Qiu *et al.*, 2014). A KOE SST index based on oxygen isotopes from California speleothems identified a 22-year periodicity that was attributed to possible solar influences on North Pacific climate (McCabe-Glynn *et al.*, 2013). SSTs from near Enoshima, off the coast of Japan (38.4°N, 141.5°E) are a useful proxy for the OC that runs southward along the Japanese coast (Figure 2, Table 2), and feature bidecadal to pentadecadal variability (Minobe, 1997, 1999) which are also observed in the PDO (Mantua *et al.*, 1997; Minobe, 1997; Yasuda *et al.*, 2006) and related reconstructions for western North America (Wilson *et al.*, 2007). We can further examine the frequency-dependent spatial structure of the relationship between reconstructed Nemuro temperatures and Pacific SSTs. Figure 6(a) shows the correlation between our reconstruction and SSTs (coloured shading) as well as the PDO-SST correlation (contours). As in Figure 2, it is clear these two correlation patterns are spatially distinct. A decadal timescales (reconstruction and SST field smoothed with 11-year lowpass Butterworth filter), the correlation between reconstructed Nemuro is more strongly zonal, and the 'horseshoe' shape of the PDO mode disappears. The structure of the zonal correlation pattern occurs along the boundary of the KOE.

4. Conclusions

We have described a new temperature reconstruction for a climatically sensitive, remote region of the western North Pacific. Results indicate that coastal land areas of northeast Asia feature distinct information relative to the eastern side of the basin. This overall finding is illustrated by the significant agreement between the Nemuro reconstruction and large-scale indices (SST, KOE, Arctic Front and Okhotsk High) of regional scale circulation (Table 2). Specifically, it is noteworthy that the correlation structure in Figure 6 between Nemuro temperatures and SST changes sign in the general region of the Oyashio–Kuroshio frontal boundary and currents, possibly indicating that Nemuro temperatures might be an indicator of frontal position and atmospheric circulation related to this primary centre of action (Nonaka *et al.*, 2006). We note that our reconstruction is based on summer temperatures and appears to express a combination of local scale variability and large-scale dynamics. Twentieth century regime shifts, as seen more clearly in the northeast Pacific instrumental PDO and PDO reconstructions (e.g. D'Arrigo *et al.*, 2001; Gedalof and Smith, 2001), tend to be more muted in summer, and in the far western north Pacific. There is some high-frequency

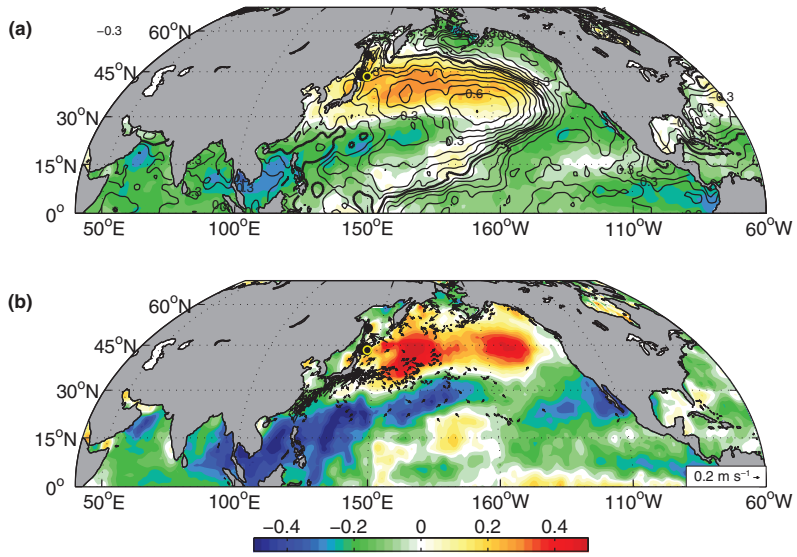

Figure 6. (a) Correlation (colour shading) between Nemuro (NEM) temperature reconstruction and JJAS HadISST (1870–1993; Rayner *et al.* 2003). Pointwise field correlation values larger than ±0.19 are significant at the $p < 0.10$ level. Overlying line contours show the correlation (1900–2012) between the JJAS PDO index and SSTs, and demonstrates that there are differences in the spatial correlation structure between PDO/SST and the NEM reconstruction/SST. The contour interval is 0.1; (b) 11-year low pass correlations between reconstruction and JJAS HadISST (Rayner *et al.* 2003), showing considerable decadal regional zonal structure likely linked to position of Oyashio/Kuroshio frontal and current dynamics, rather than the PDO. Pointwise field correlation values larger than ±0.42 are significant at the $p < 0.10$ level following the method described by Ebisuzaki (1997). Also shown are JJAS North Pacific (north of 20°N) mean surface current velocities from Lumpkin and Johnson (2013). Only surface currents with zonal and meridional components greater than 0.1 m s^{-1} are plotted.

coherence with the PDO in our summer record, but with distinct decadal differences relative to those expressed over western North America, indicating spatial complexity. The robust quasi-bidecadal peaks at Nemuro appear to correspond more to regional features of western North Pacific coupled atmosphere–ocean processes, and specifically to Kuril and KOE-related SST anomalies in the western North Pacific. Effects of intense mixing can include anomalous SSTs and sea fog in the Okhotsk Sea in summer (Tokinaga and Xie, 2009), which could impact forest growth via cooler temperatures and decreased incoming solar radiation. Understanding of air–sea interactions in the northwest Pacific Ocean and greater basin are still not well understood. In particular one question is whether or not low-frequency variability associated with the ENSO system in the tropics is the cause of decadal to longer-term variations at higher latitudes (e.g. Allan, 2000; Deser *et al.*, 2004). An alternative explanation might be related to air–sea exchanges on the local to regional level, but there is currently too little data for these intrinsic modes of interaction to be explored. Additional data and comparisons of proxies from around the North Pacific rim, including spatial reconstructions, will aid understanding of the long-term processes, forcing mechanisms, and spatiotemporal extent of complex climate phenomena on time scales not currently resolvable by the instrumental record.

Acknowledgements

We thank the National Science Foundation Paleoclimatology Program, Grant AGS-1159430 and AGS-1202218. We also gratefully acknowledge the ITRDB and other contributors of tree-ring data, including M. Sano of Kyoto University and K. Yasue of Shinshu University, Japan. These data are either readily available on the ITRDB or from the authors, or will be submitted to the ITRDB prior to publication of this manuscript. Lamont-Doherty Earth Observatory Contribution No. 0000.

References

Allan R. 2000. ENSO and climatic variability in the past 150 years. In *El Niño and the Southern Oscillation: Multiscale Variability and Global and Regional Impacts*, Diaz H, Markgraf V (eds). Cambridge University Press: Cambridge, UK, 3–56.

Allan R, Ansell T. 2006. A new globally complete monthly historical mean sea level pressure data set (HadSLP2): 1850-2004. *J. Clim.* **19**: 5816–5842.

Barnston AG, Livezey RE. 1987. Classification, seasonality and persistence of low-frequency atmospheric circulation patterns. *Mon. Weather Rev.* **115**: 1083–1126.

Bond N, Overland J, Spillane M, Stabeno P. 2003. Recent shifts in the state of the North Pacific. *Geophys. Res. Lett.* **30**: 2183, doi: 10.1029/2003GL018597.

Cook ER, Kairiukstis L. 1990. *Methods of Dendrochronology*. Kluwer Press: Boston, MA.

Cook E, D'Arrigo R, Mann M. 2002. A well-verified, multiproxy reconstruction of the winter North Atlantic Oscillation index since AD 1400. *J. Clim.* **15**: 1754–1764.

Cook E, Krusic P, Anchukaitis K, Buckley B, Nakatsuka T, Sano M. 2012. Tree-ring reconstructed summer temperature anomalies for temperate East Asia since 800 C.E. *Clim. Dyn.* **41**: 2957–2972, doi: 10.1007/s00382-012-1611-x.

D'Arrigo R, Wilson R. 2006. On the Asian expression of the PDO. *Int. J. Climatol.* **26**: 1607–1617, doi: 10.1002/joc.1326.

D'Arrigo R, Yamaguchi D, Wiles G, Jacoby G, Osawa A, Lawrence D. 1997. A Kashiwa oak (*Quercus dentata*) tree-ring width chronology from northern coastal Hokkaido, Japan. *Can. J. For. Res.* **27**: 613–617.

D'Arrigo R, Villalba R, Wiles G. 2001. Tree-ring estimates of Pacific decadal climate variability. *Clim. Dyn.* **18**: 219–224.

D'Arrigo R, Wilson R, Deser C, Wiles G, Cook E, Villalba R, Tudhope A, Cole J, Linsley B. 2005. Tropical-North Pacific climate linkages over the past four centuries. *J. Clim.* **18**: 5253–5265.

Davi N, D'Arrigo R, Jacoby G, Buckley B, Kobayashi O. 2001. Warm-season annual to decadal temperature variability for Hokkaido, Japan reconstructed from tree-ring density data: AD 1557–1990. *Clim. Change* **52**: 201–217.

Dawdy D, Matalas N. 1964. Statistical and probability analysis of hydrologic data, part III: Analysis of variance, covariance and time series. In *Handbook of Applied Hydrology, a Compendium of Water-Resources Technology*, Chow VT (ed). McGraw-Hill Book Company: New York, NY, 8.68–8.90.

Deng W, Gangjian W, Xie L, Ke T, Wang Z, Zeng T, Liu Y. 2013. Variations in the Pacific Decadal Oscillation since 1853 in a coral record from the northern South China Sea. *J. Geophys. Res. Oceans* **118**: 2358–2366, doi: 10.1002/jgrc.20180.

Deser C, Phillips A, Hurrell J. 2004. Pacific interdecadal climate variability: linkages between the tropics and North Pacific during boreal winter since 1900. *J. Clim.* **17**: 3109–3124.

Ebisuzaki W. 1997. A method to estimate the statistical significance of a correlation when the data are serially correlated. *J. Clim.* **10**: 2147–2153.

Frauenfeld O, Davis R. 2002. Midlatitude circulation patterns associated with decadal and interannual Pacific Ocean variability. *Geophys. Res. Lett.* **29**: 2221, doi: 10.1029/2002GL015743.

Gedalof Z, Smith D. 2001. Interdecadal climate variability and regime-scale shifts In Pacific North America. *Geophys. Res. Lett.* **28**: 1515–1518.

Hasumi H, Yasuda I, Tatebe H, Kimoto M. 2008. Pacific bidecadal climate variability regulated by tidal mixing around the Kuril Islands. *Geophys. Res. Lett.* **35**: L14601, doi: 10.1029/2008GL034406.

Jacoby G, Solomina O, Frank D, Eremenko N, D'Arrigo R. 2004. Kunashir (Kuriles) oak 400-year reconstruction of temperature and relation to the Pacific Decadal Oscillation. *Palaeogeogr. Palaeoclimatol. Palaeoecol.* **209**: 303–311.

Kennedy J, Rayner N, Smith R, Saunby M, Parker D. 2011. Reassessing biases and other uncertainties in sea-surface temperature observations since 1850 part 1: measurement and sampling errors. *J. Geophys. Res.* **116**: D14103, doi: 10.1029/2010JD015218.

Kwon Y, Deser C. 2007. North Pacific decadal variability in the Community Climate System Model Version 2. *J. Clim.* **20**: 2416–2433.

Lumpkin R, Johnson G. 2013. Global ocean surface velocities from drifters: mean, variance, ENSO response, and seasonal cycle. *J. Geophys. Res. Oceans* **118**: 2992–3006, doi: 10.1002/jgrc.20210.

Mann M, Lees J. 1996. Robust estimation of background noise and signal detection in climatic time series. *Clim. Change* **33**: 409–445.

Mantua N, Hare S, Zhang Y, Wallace J, Francis R. 1997. A Pacific interdecadal climate oscillation with impacts on salmon production. *Bull. Am. Meteorol. Soc.* **78**: 1069–1080.

McCabe-Glynn S, Johnson K, Strong C, Berkelhammer M, Sinha A, Cheng A, Lawrence Edwards R. 2013. Variable North Pacific influence on drought in southwestern North America since 854. *Nat. Geosci.* **6**: 617–621, doi: 10.1038/NGEO1862.

Minobe S. 1997. A 50–70 year climatic oscillation over the North Pacific and North America. *Geophys. Res. Lett.* **24**: 683–686.

Minobe S. 1999. Resonance in bidecadal and pentadecadal climate oscillations over the North Pacific: role in climatic regime shifts. *Geophys. Res. Lett.* **26**: 855–858.

Morice C, Kennedy J, Rayner N, Jones P. 2012. Quantifying uncertainties in global and regional temperature change using an ensemble of observational estimates: The HadCRUT4 dataset. *J. Geophys. Res.* **117**: D08101, doi: 10.1029/2011JD017187.

Nakamura H, Lin G, Yamagata T. 1997. Decadal climate variability in the North Pacific during the recent decades. *Bull. Am. Meteorol. Soc.* **78**: 2215–2224.

Nakamura H, Izumi T, Sampe T. 2002. Interannual and decadal modulations recently observed in the Pacific storm track activity and East Asian winter monsoon. *J. Clim.* **15**: 1855–1874.

Newman M. 2007. Interannual to decadal predictability of tropical and North Pacific sea surface temperatures. *J. Clim.* **20**: 2333–2355.

Nonaka M, Nakamura H, Tanimoto Y, Kagimoto T, Sasaki H. 2006. Decadal variability in the Kuroshio-Oyashio Extension simulated in an eddy-resolving OGCM. *J. Clim.* **19**: 1970–1989.

Ogi M, Tachibana Y, Yamazaki K. 2004. The connectivity of the winter North Atlantic Oscillation (NAO) and the summer Okhotsk High. *J. Meteorol. Soc. Japan* **82**: 905–913.

Ohyama M, Yonenobu H, Choi J, Park W, Hanzawa M, Suzuki M. 2013. Reconstruction of northeast Asia spring temperature 1784-1990. *Clim. Past* **9**: 261–266.

Osafune S, Yasuda I. 2006. Bidecadal variability in the intermediate waters of the northwestern subarctic Pacific and the Okhotsk Sea in relation to 18.6-year period nodal tidal cycle. *J. Geophys. Res.* **111**(C5): C05007, doi: 10.1029/2005JC003277.

Peterson T, Vose R. 1997. An overview of the Global Historical Climatology Network (v.2) temperature data base. *Bull. Am. Meteorol. Soc.* **78**: 2837–2849.

Pierce D, Barnett T, Schneider N, Saravanan R, Dommenget D, Latif M. 2001. The role of ocean dynamics in producing decadal climate variability in the North Pacific. *Clim. Dyn.* **18**: 51–70.

Qiu B, Chen S, Schneider N. 2014. A coupled decadal prediction of the dynamic state of the Kuroshio Extension system. *J. Clim.* **27**: 1751–1764.

Rayner N, Parker D, Horton E, Folland C, Alexander L, Rowell D, Kent E, Kaplan A. 2003. Global analyses of sea surface temperature, sea ice, and night marine air temperature since the late nineteenth century. *J. Geophys. Res.* **108**(D14): 4407, doi: 10.1029/2002JD002670.

Sano M, Furuta F, Sweda T. 2010. Summer temperature variations in southern Kamchatka as reconstructed from a 247-year tree-ring chronology of *Betula ermanii*. *J. For. Res.* **15**: 234–240.

Schneider N, Cornuelle B. 2005. The forcing of the Pacific Decadal Oscillation. *J. Clim.* **18**: 4355–4373, doi: 10.1175/JCLI3527.1.

Shen C, Wang W, Gong W, Hao Z. 2006. A Pacific decadal oscillation record since 1470 AD reconstructed from proxy data of summer rainfall over eastern China. *Geophys. Res. Lett.* **33**: L03702, doi: 10.1029/2005GLO24804.

Solomina O, Wiles G, Shiraiwa T, D'Arrigo R. 2007. Multiproxy records of climate variability for Kamchatka for the past 400 years. *Clim. Past* **3**: 119–128.

Tanaka Y, Yasuda I, Hasumi H, Tatebe H, Osafune S. 2012. Effects of the 18.6 year modulation of tidal mixing on the North Pacific bidecadal climate variability in a coupled climate model. *J. Clim.* **25**: 7625–7642.

Thompson D, Wallace J. 1998. The Arctic Oscillation signature in the wintertime geopotential height and temperature fields. *Geophys. Res. Lett.* **25**: 1297–1300.

Thomson D. 1982. Spectrum estimation and harmonic analysis. *Proc. IEEE* **70**: 1055–1096.

Tokinaga H, Xie S. 2009. Ocean tidal cooling effect on summer sea fog over the Okhotsk Sea. *J. Geophys. Res.* **114**: D14102, doi: 10.1029/2008JD011477.

Wang C, Deser C, Yu J, DeNezio P, Clement A. 2012a. El Nino and Southern Oscillation: a review. In *Coral Reefs of the Eastern Pacific*. Springer-Verlag.: Berlin, 3–19.

Wang R, Dearling J, Langdon P, Zhang E, Yang X, Dakos V, Scheffer M. 2012b. Flickering gives early warning signals of a critical transition to a eutrophic lake state. *Nature* **492**: 419–422.

Wiles G, D'Arrigo R, Jarvis S, Barclay D, Appleton S, Wilson R, Frank D, Lawson D. 2014a. Surface air temperature variability for the Gulf of Alaska over the past 1200 years. *Holocene* **24**: 198–208, doi: 10.1177/0959683613516815.

Wiles G, Solomina O, D'Arrigo R, Anchukaitis K, Gensiarovsky Y, Wiesenberg N. 2014b. Reconstructed summer temperatures over the last 400 years based on larch ring widths: Sakhalin Island, Russian Far East. *Clim. Dyn.*, doi: 10.1007/s00382-014-2209-2.

Wilson R, Wiles G, D'Arrigo R, Zweck C. 2007. Cycles and shifts: 1300 years of multi-decadal temperature variability in the Gulf of Alaska. *Clim. Dyn.* **28**: 425–440, doi: 10.1007/s00382-006-0194-9.

Yasuda I, Osafune S, Tatebe H. 2006. Possible explanation linking 18.6-year period nodal tidal cycle with bi-decadal variations of ocean and climate in the North Pacific. *Geophys. Res. Lett.* **33**: L08606, doi: 10.1029/2005GL025237.

